Proceedings of the ASME 2021 International Technical Conference and Exhibition on Packaging and Integration of Electronic and Photonic Microsystems
InterPACK2021
October 26-28, 2021, Virtual, Online

IPACK2021- 73283

THERMAL-HYDRAULIC ANALYTICAL MODELS OF SPLIT-FLOW MICROCHANNEL LIQUID-COOLED COLD PLATES WITH FLOW IMPINGEMENT

Deogratius Kisitu[1], Alfonso Ortega[1]
[1]Laboratory for Advanced Thermal and Fluid Systems
Department of Mechanical Engineering
Villanova University, Villanova, PA 19085, USA

ABSTRACT

Impingement split flow liquid-cooled microchannel cold plates are one of several flow configurations used for single-phase liquid cooling. Split flow or top-in/side-exit (TISE) cold plates divide the flow into two branches thus resulting in halved or reduced flow rates and flow lengths, compared to traditional side-in /side-exit (SISE) or parallel flow cold plates. This has the effect of reducing the pressure drop because of the shorter flow length and lower flow rate and increasing the heat transfer coefficient due to thermally developing as opposed to fully developed flow. It is also claimed that the impinging flow increases the heat transfer coefficient on the base plate in the region of impingement. Because of the downward impinging and turning flow, there are no exact analytical models for this flow configuration. Computational and experimental studies have been performed, but there are no useful compact analytical models in the literature that can be used to predict the performance of these impingement cold plates. Results are presented for novel physics-based laminar flow models for a TISE microchannel cold plate based on an equivalent parallel channel flow approach. We show that the new models accurately predict the thermal-hydraulic performance over a wide range of parameters.

Keywords: Impingement, Microchannel cold plates, Liquid Cooling, Analytical models, Thermal-hydraulic performance

NOMENCLATURE

A	Area, m^2
b	Channel width, m
c_p	Specific heat, J/kgK
D_h	Channel hydraulic diameter, m
f	Fanning friction factor
$\bar{h}$	Average heat transfer coefficient, $\mathrm{W/m^2K}$
H	Height, m
k	Thermal conductivity, W/mK
K_c	Contraction coefficient
K_e	Expansion coefficient
L	Base plate length, m
l_{eff_1}	Effective length of the vertical channel, m
l_{eff_2}	Effective length of the horizontal channel, m
L_{eff}	Proposed total effective flow length, m
L_h	Hydrodynamic entrance length, m
L_{th}	Thermal entrance length, m
$\dot{m}$	Mass flow rate, kg/s
N	Number of channels
NTU	Number of transfer units
$\overline{Nu}$	Average Nusselt number
Pr	Prandtl number
P	Pressure, Pa
$\dot{q}$	Total heat transfer rate, W
q''	Heat flux, W/cm^2
Re	Reynolds number
R	Thermal resistance, K/W
t	Fin thickness, m
T	Temperature, K
U	Average velocity, m/s
W	Width, m
x^+	Dimensionless hydrodynamic channel length
x^*	Dimensionless thermal channel length

Greek Symbols

α	Channel aspect ratio
β	Jet slot aspect ratio
ε	Effectiveness of a cold plate
σ	Fin array porosity
θ	Tilt angle, °
ρ	Density, $\mathrm{kg/m^3}$
η_{fin}	Fin efficiency
η_o	Overall surface efficiency
ΔP	Pressure drop, Pa
ν	Kinematic viscosity, $\mathrm{m^2/s}$
μ	Dynamic viscosity, Pa s

Subscripts

avg	Area-averaged
B	Base
$chan$	Channel
$cond$	Conductive
cop	Copeland
c	Chip
cp	Cold plate
eff	Effective
fin	Fin
fd	Fully-developed
hd	Hydrodynamically-developing
j	Jet
liq	Liquid
m	Bulk mean
i	Inlet
o	Outlet
S	SISE
s	Solid
sp	Spreading
tot	Total
T	TISE
w	Wall

1. INTRODUCTION

The advent of high-performance electronics, including central processing units (CPU's), graphic processing units (GPU's) and others, is steadily increasing the heat loads to be handled. The air-cooling limits are now being exceeded. Indirect liquid cooling, with water or water/glycol fluids such as 25% propylene glycol coolant, has emerged as a powerful thermal management solution to dissipate high heat fluxes, which cannot be cooled with air. In the indirect approach, the coolant liquid is circulated through extended surface heat sinks, more generally referred to as "cold plates" when used with single-phase liquids, that are attached to the package lid with an intermediary thermal interface material. Impingement split flow or top-in/side-exit (TISE) microchannel cold plates are among the heat sinks deployed in indirect liquid cooling. Unlike for the side-in/side-exit (SISE) microchannel cold plates, there are no analytical thermal-hydraulic models for split flow/TISE microchannel cold plates because of flow turning physics. Some pertinent previous investigations, regarding the split flow configuration, are briefly reviewed.

Several attempts were made to model impingement air-cooled macrochannel heat sinks. Duan and Muzychka [1] experimentally investigated the hydraulic and thermal performance of split flow macrochannel air-cooled heat sinks and proposed thermal-hydraulic models based on a developing laminar flow in rectangular channels. They obtained good agreement between the proposed analytical models and experimental data. Kang and Holahan [2] suggested a 1-D model of an impingement macrochannel heat sink with assumption of air flow from the fin tips to the fin base, and developed a CFD model, whose results agreed with experimental data. Correlations were then proposed for the heat sink thermal resistance and pressure drop. Holahan et al [3] proposed an analytical model for laminar flow impingement air-cooled heat sink to predict the thermal-hydraulic performance using Hele-Shaw flow in the channel between the fins. The conduction fin model was derived basing on superposition of a Kernel function developed from the method of images. Biber [4] conducted numerical studies and analytical scaling to estimate the thermal-hydraulic performance of single isothermal air-cooled split flow macrochannels with varying jet inlet-widths. Dimensionless thermal-hydraulic models/correlations were proposed for TISE configuration heat sinks from numerical simulation results. Issa and Ortega [5] conducted an experimental study on the hydraulic and heat transfer performance of jet impingement pin fin air-cooled heat sinks. They found that the overall thermal resistance reduced by increasing the Reynolds number, pin density and pin diameter. The thermal resistance is a function of pin height and clearance ratio at low Reynolds numbers, and is a weak function of the same at high Reynolds numbers. Gutiérrez and Ortega [6] experimentally measured static pressure and temperature in fine pitch impingement macrochannel copper air-cooled heat sinks with and without top bypass flow. A set of these heat sinks with differing fin pitch, with and without anodized finish were also examined in a cross-flow wind tunnel that provides zero to one top clearance ratio.

Sung and Mudawar [7] investigated single-phase cooling performance of a split flow microchannel module using HFE-7100 as a coolant. 3-D numerical simulations were performed to both investigate single-phase performance and optimize the geometry to maximize heat removal and surface temperature uniformity while reducing mean surface temperature. Experimental studies followed to validate the numerical findings and aid in the development of correlations for single-phase heat transfer coefficients.

There have been relatively few studies for split flow microchannel cold plates with liquid flow. Hadad et al. [8] performed numerical modelling of a warm water-cooled microchannel V-grooved impinged (TISE) cold-plate to predict pressure drop and thermal performance and conducted optimization. They also investigated the effects of fin tilt angle on pressure drop and thermal resistance using numerical modeling. They observed that the pressure drop increases with tilt angle and that thermal resistance is a weak function of the same. In a related study, Hadad et al. [9] developed a numerical model including the effects of inlet and outlet manifolds (distributor and collector) on the impingement microchannel cold plate hydraulic and thermal performance. Their CFD model was utilized in shape optimization of the split flow cold plate. Ramakrishnan et al. [10] experimentally characterized a commercially available split flow microchannel cold plate, which uses warm water in cooling the chip. The thermo-hydraulic performance of the split flow cold plates was investigated experimentally, and a resistance network model was used to calculate an effective heat transfer coefficient.

In summary, there is little or no work in the literature, pertinent to useful approximate compact analytical thermal-hydraulic models for predicting the performance of split flow or jet impingement liquid-cooled microchannel cold plates. These compact models can be used by thermal engineers for estimation of the performance of split flow cold plates without the need of costly, complex CFD simulation. The current work focuses on developing and validating approximate physics-based analytical models for the TISE or split flow cold plates used in single-phase indirect liquid cooling. The analytical modeling of these split flow microchannel cold plates is simplified using an equivalent parallel flow (SISE) configuration concept.

2. DEVELOPMENT OF COMPACT MODELS FOR SPLIT FLOW MICROCHANNEL COLD PLATES

In this section, we present an equivalent parallel flow (SISE) concept as the basis for new split flow compact models and develop the modeling equations for thermal resistance and pressure drop.

2.1 Equivalent parallel flow (SISE) concept

Considering symmetry, it is hypothesized that a generic impingement split flow or TISE liquid-cooled half microchannel can be treated and modeled as an equivalent parallel flow (SISE) microchannel configuration, which has an effective total flow length, L_{eff}, as shown in Fig. 1. Finding a definition for L_{eff} is at the heart of this proposed model.

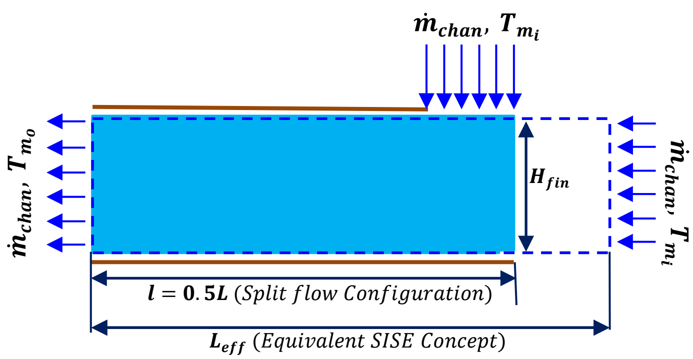

FIGURE 1: SPLIT FLOW AND EQUIVALENT SISE CONCEPT

In previous work, for air-cooled impingement split flow macrochannel heat sinks, Duan and Muzychka [1] considered an L-shaped streamline as shown in Fig. 2. They treated the turning flow as vertical and horizontal channels connected at a right angle, and defined effective flow lengths for both channels, as given in Eqns. 1 and 2, respectively.

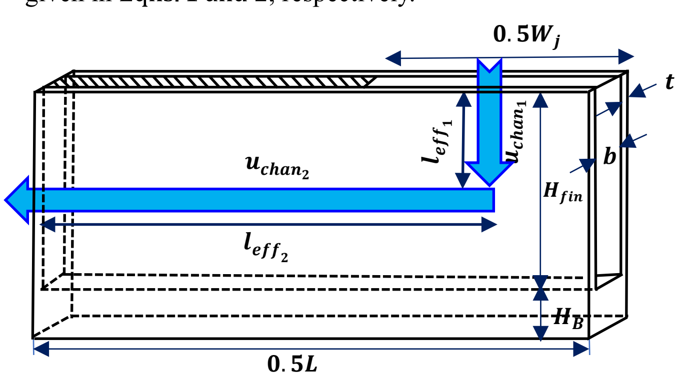

FIGURE 2 : DUAN AND MUCHYKA MODEL – AIR COOLED HEAT SINK

$$l_{\text{eff}_1} = 0.5H_{fin} \tag{1}$$

$$l_{\text{eff}_2} = 0.5L - 0.25W_j \tag{2}$$

It is clear that the definitions for l_{eff_1} and l_{eff_2} are purely intuitive. Duan and Muchyka distinctly modeled the flow and heat transfer for each of these two channels. In the currently proposed concept, a total effective flow length, L_{eff} is defined as the arithmetic sum of the two effective flow lengths – l_{eff_1} *and* l_{eff_1} – in the Duan and Muchyka model, as given in Eqn. 3. This means L_{eff} is considered the flow length of the equivalent parallel flow (SISE) microchannel unit cell that is currently theorized to be equivalent to the symmetric or half split flow microchannel unit cell, in terms of thermal resistance and pressure drop.

$$L_{\text{eff}} = l_{\text{eff}_1} + l_{\text{eff}_2} \tag{3}$$

A vital parameter in split flow cold plates modeling is the jet slot aspect ratio, β, which refers to the ratio of the jet slot width to the total length of the cold plate, is defined as;

$$\beta = {}^{W_j}/_{L} \tag{4}$$

Substituting Eqns. 1, 2 and 4 into Eqn. 3, and simplifying, L_{eff} can then be expressed as a function of $L,\ \beta$ *and* H_{fin}.

$$L_{\text{eff}} = 0.5\left[(1 - 0.5\beta)L + H_{fin}\right] \tag{5}$$

2.2 Derivation of Thermal-hydraulic Compact Models

2.2.1 Proposed Isothermal Model

Based on the proposed equivalent SISE concept, the $\bar{h}$ for split flow cold plate is modeled as laminar flow in an isothermal SISE (parallel flow) rectangular microchannel. The total thermal resistance for the split flow cold plate is derived following a rigorous approach.

Modeling Assumptions

The following assumptions were taken during thermal analytical modeling of the split flow microchannel cold plate;

1. Constant properties of the coolant and substrate
2. Steady-state heat transfer
3. Isothermal microchannels, and adiabatic fin tips.
4. Negligible axial heat conduction in the coolant and substrate
5. Negligible radiation heat transfer and heat generation

Modeling Film Coefficient, $\bar{h}$ for Split Flow Cold Plates

The thermal entrance length, $l_{th,}$ for a half TISE or split flow microchannel unit cell is given as [11];

$$l_{th} = 0.1Re_{D_h}D_hPr \tag{6}$$

The channel aspect ratio for split flow cold plate microchannels is given by;

$$\alpha = \frac{H_{fin}}{b} \tag{7}$$

In the present analysis, the hydraulic diameter, D_h is defined as a function of θ_{fin}, to include the effects of tilted fins on performance. Fin tilting was previously investigated using numerical and experimental approaches [8], on such tilted-fin impingement cold plates, such as those from CoolIT^{TM}. For low α and tilted fins, D_h may be defined as given in Eqn. 8.

$$D_h = \frac{2b \sin \theta_{fin}}{\left(1 + \frac{1}{\alpha} \sin \theta_{fin}\right)} \quad for \;\; 0° < \theta_{fin} \leq 90° \tag{8}$$

And, for high $\alpha's$ and vertical fins, D_h in reduces to;

$$D_h = 2b \qquad for \;\; \theta_{fin} = 90°, \qquad \alpha >> 1 \tag{9}$$

The channel Reynolds number is expressed as below;

$$Re_{D_h} = \frac{U_{chan} D_h}{v_{liq}} \tag{10}$$

From continuity, channel velocity can be expressed as a function of jet velocity;

$$U_{chan} = \left(\frac{W_j}{H_{fin}}\right) * U_j \tag{11}$$

Combining Eqns. 10 and11 gives;

$$Re_{D_h} = \left(\frac{U_j D_h}{v_{liq}}\right)\left(\frac{W_j}{H_{fin}}\right) \tag{12}$$

The dimensionless thermal length in a half split flow microchannel unit cell is given as a function of L_{eff}, from the proposed equivalent parallel flow (SISE) concept.

$$x^*_{eff} = \frac{\left(L_{eff}/D_h\right)}{Re_{D_h} Pr} \tag{13}$$

The average heat transfer coefficient, $\bar{h}$, based on the bulk mean fluid temperature, is defined as;

$$\bar{h} = \frac{1}{L_{eff}} \int_0^{L_{eff}} h(x)dx = \frac{1}{L_{eff}} \int_0^{L_{eff}} \left(\frac{q''_x}{[T_w - T_b(x)]}\right) dx \tag{14}$$

$\bar{h}$ can also be defined as a function of $\overline{Nu}$;

$$\bar{h} = \overline{Nu}\left(\frac{k_{liq}}{D_h}\right) \tag{15}$$

The simplicity of the current thermal analytical model is that known correlations and models for determining $\overline{Nu}$ for laminar flow in rectangular SISE microchannels can be used in the thermal analysis of the impingement split flow or TISE microchannel liquid-cooled cold plates.

An appropriate correlation, for developed and developing laminar flow in isothermal channels, for predicting $\overline{Nu}$ based on mixed mean fluid temperature, proposed by Copeland (2000) [12], as given by $Eqn. 16$, can be applied in this modeling.

$$\overline{Nu} = \left\{\left[2.22\left(x^*_{eff}\right)^{-0.33}\right]^3 + \left(\overline{Nu}_{fd,cop}\right)^3\right\}^{1/3} \tag{16}$$

Where,

$$\overline{Nu}_{fd,cop} = 8.31G - 0.02 \tag{17}$$

$$G = \frac{[(1/\alpha)^2 + 1]}{[1/\alpha + 1]^2} \tag{18}$$

$Eqns. 15 - 18$ can be used to predict $\bar{h}$ for a split flow microchannel cold plate.

Modeling Thermal Resistance for Split Flow Cold Plate

In this analysis, the thermal resistance of a split flow cold plate is derived from the proposed equivalent SISE concept by taking an energy balance – as illustrated below in Fig. 3 – on the control volume of the coolant (liquid) in an equivalent parallel flow (SISE) rectangular isothermal microchannel.

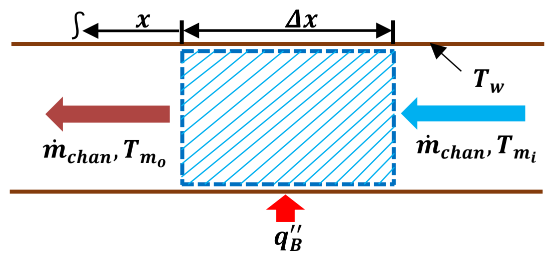

FIGURE 3: ENERGY BALANCE ON A LIQUID CONTROL VOLUME

For a split flow cold plate, with N_T full split flow microchannels or with N_S or $2N_T$ proposed equivalent SISE (parallel flow) microchannels, the overall thermal resistance model of the split flow or TISE cold plate was derived [13], which is a function of heat exchanger effectiveness (ε_T), given by $Eqn. 19$, and is similar to a model proposed by Copeland for air-cooled heat sinks [12]

$$R_{cp} = \frac{1}{\dot{m}_{cp} c_p \varepsilon_T} = \frac{1}{\dot{m}_{cp} c_p (1 - e^{-NTU_T})} \tag{19}$$

Where,

$$NTU_T = \frac{\eta_{o,T} A_{w,T} \bar{h}}{\dot{m}_{cp} c_p} \tag{20}$$

$$A_{w,T} = N_{fin}.\left(2H_{fin}.(L_T + t)\right) + N_T.b.L_T \tag{21}$$

$$L_T = 2L_{\text{eff}} \tag{22}$$

$$\eta_o = 1 - \frac{2A_f}{A_{w,T}}\left(1 - \eta_{fin}\right) \tag{23}$$

$$\dot{m}_{cp} = N_S.\dot{m}_{chan} \tag{24}$$

The base plate conductive thermal resistance of the split flow cold plate is be given by;

$$R_{cond} = \frac{H_B}{k_B A_B} \tag{25}$$

Where,

$$A_B = W_B.L \tag{26}$$

In some electronic cooling cases, the chip/source footprint area, A_c is less than the cold plate base footprint area, A_B. To account for the heat spreading in the cold plate base, the spreading thermal resistance in a split flow cold plate is computed from a correlation by Lee [14], given by $Eqn. 27$.

$$R_{sp} = \frac{\left(\sqrt{A_B} - \sqrt{A_c}\right)}{k_B\sqrt{\pi A_B A_c}} \frac{\left(\lambda k_B A_B R_{cp} + \tanh(\lambda H_B)\right)}{\left(1 + \lambda k_B A_B R_{cp} \tanh(\lambda H_B)\right)} \quad (27)$$

Where,

$$\lambda = \frac{\pi^{1.5}}{\sqrt{A_B}} + \frac{1}{\sqrt{A_c}} \quad (28)$$

The total split flow cold plate thermal resistance can be modeled by summing all the aforecited thermal resistances;

$$R_{tot} = R_{cp} + R_{cond} + R_{sp} \quad (29)$$

Substituting Eqns. 19, 25 and 27 into Eqn. 29, gives the final expression of the total thermal resistance of a TISE (jet impingement) microchannel liquid-cooled cold plate.

2.2.2 Proposed Hydraulic Model

Based on the proposed equivalent SISE concept, the pressure drop of a split flow cold plate is a function of the total effective length (L_{eff}), channel velocity, and the Fanning friction factor for the equivalent SISE rectangular channels [15].

Modeling Assumptions

The following assumptions were taken during hydraulic analytical modeling of split flow microchannel cold plates;

1) Steady-state flow
2) Incompressible and Newtonian fluid
3) Constant property liquid
4) Hydrodynamically developed laminar flow.

Modeling Friction Factor, f for Split Flow Cold Plates

For split flow cold plate channels, the coefficient of friction, f can be modeled as that for rectangular equivalent parallel flow (SISE) channels. Copeland [12] developed an appropriate model for f for fully developed laminar flow in rectangular SISE channels and is a function of channel aspect ratio.

$$f = \frac{(19.64G + 4.7)}{Re_{D_h}} \quad (30)$$

Modeling Pressure Drop for Split Flow Cold Plates

The pressure drop in split flow cold plate microchannels can be modeled as that for a single equivalent SISE (parallel flow) rectangular microchannel, basing on the proposed concept, and such models are available in the literature [15]. In this modeling, the pressure drop for split flow cold plate is a function of L_{eff}.

The hydrodynamic entrance length, l_h, for liquid flow in the symmetric or half split flow microchannel is given by [11], and aids to determine if flow is hydrodynamically developed, or not.

$$l_h = 0.056 Re_{D_h} D_h \quad (31)$$

And the dimensionless streamwise coordinate – which is a function of the of the proposed L_{eff} – is given by;

$$x^{+}{}_{eff} = \left(\frac{L_{\text{eff}}}{D_h}\right) / Re_{D_h} \quad (32)$$

For fully developed laminar flow through a split flow microchannel cold plate, the pressure drop ΔP_{CP}, is modeled as sum of entrance and exit losses, and the core frictional losses [11], as given in Eqns. 33

$$\Delta P_{cp} = \frac{\rho_{liq} u_{chan}^2}{2}\left[\frac{4 f L_{\text{eff}}}{D_h} + (K_c + K_e)\right] \quad (33)$$

From Kays and London [15], the contraction (K_c) and expansion (K_e) loss coefficients due to area changes, for high aspect ratio – are functions of fin array porosity (σ).

$$\sigma = \frac{b}{b+t} \quad (34)$$

$$K_c = 0.8 - 0.4\sigma^2 \quad (35)$$

$$K_e = 1.0(1-\sigma)^2 - 0.4\sigma \quad (36)$$

If the flow were hydrodynamically developing and laminar, the apparent friction factor could be modeled as [12];

$$f_{hd} = \frac{\left[\left(3.2\left(x_{eff}^{+}\right)^{-0.57}\right)^2 + (f Re_{Dh})^2\right]^{0.5}}{Re_{Dh}} \quad (37)$$

2.3 Numerical Modeling

2.3.1 Assumptions

In the present numerical modeling, the following key assumptions are taken.

1) The flow is 3-D and laminar.
2) Negligible effects of gravity and other body forces.
3) Constant thermo-physical properties of copper and water
4) Constant heat flux at the base.
5) Identical microchannels, both thermally and hydraulically, and thus, a single half split flow microchannel can be considered as a computational domain due to symmetry.

2.3.2 Governing Equations

The governing equations for a conjugate heat transfer problem in an incompressible steady-state laminar flow regime are;

1. Conservation of mass (continuity) for liquid (water)

$$\nabla . \vec{V} = 0 \quad (38)$$

2. Equations of motion for liquid (water)

$$\rho_{liq}\left(\vec{V}.\nabla\right)\vec{V} = -\nabla P + \mu_{liq}\nabla^2\vec{V} \quad (39)$$

3. Energy Equation for liquid (water)

$$\rho_{liq} c_{p,liq}\left(\vec{V}.\nabla\right)T_{liq} = k_{liq}\nabla^2 T_{liq} \quad (40)$$

4. Energy Equation for solid (copper)

$$\nabla^2 T_s = 0 \quad (41)$$

2.3.3 Numerical Method

In all the current computational fluid dynamics (CFD) modeling cases, ANSYS/Fluent 3-D simulations were conducted. Semi-Implicit Method for Pressure Linked Equations (SIMPLE) algorithm, which is a Patankar's finite volume method, was applied to numerically solve the governing equations (Navier-Stokes equations). A second-order upwind scheme was applied in the discretization of the Navier-Stokes equations and energy equation. A grid independence analysis is performed based on unit thermal resistance and pressure drop (the difference between the area-averaged pressures on the inlet and the outlet of the symmetric split flow microchannels) defined by Eqns. 42 and 43, respectively.

$$R_{th} = \frac{(T_{B,max} - T_{m_i})}{q''_B} \tag{42}$$

$$\Delta P = P_{avg,i} - P_{avg,o} \tag{43}$$

2.3.4 CFD Model Validation

Due to the scarcity of experimental data in literature, a CFD model was developed and validated against the available data from [8]. The CFD simulation results were then used to validate the analytical model.

An impingement or split flow water-cooled microchannel cold plate, with full details of the geometry and flow conditions, provided by [8], was considered for CFD simulation. The unit thermal resistances and pressure drops from the current split flow cold plate CFD model were compared with Hadad et al experimental data [8] and an approximate analytical model [1].

A grid sensitivity analysis for the split flow (TISE) microchannel cold plate [8] was conducted, varying the number of cells from 93,450 to 449,304 cells, and a grid with 236,718 cells was considered for the present numerical model validation.

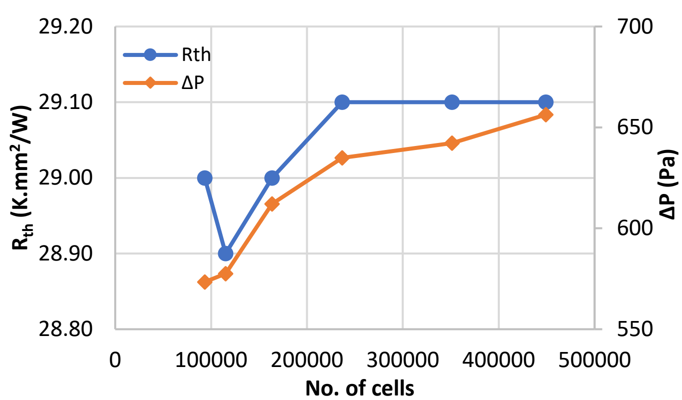

FIGURE 4: GRID INDEPENDENCE ANALYSIS FOR TISE CFD MODEL

To ensure accuracy, a special software called WebPlotDigitizer (Version 4.4) [16], was used to extract numerical data from the graphs of Hadad et al. [8].

As shown in Fig.5, there is good agreement between the unit thermal resistances from the current CFD model and experimental data [8], thus validating the present split flow thermal numerical (CFD) method.

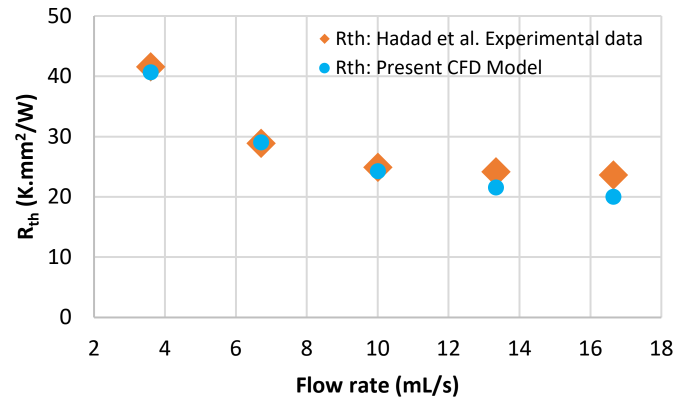

FIGURE 5: VALIDATION OF PRESENT TISE CFD MODEL (THERMAL)

Due to lack of relevant split flow pressure drop experimental data in the aforecited reference [8], an appropriate analytical model by Duan and Muzychka [1], for TISE macrochannel heat sinks, was used in CFD model validation. There is good agreement between the pressure drop from the current CFD model and the Duan and Muzychka model [1], thus validating the current split flow hydraulic numerical (CFD) method.

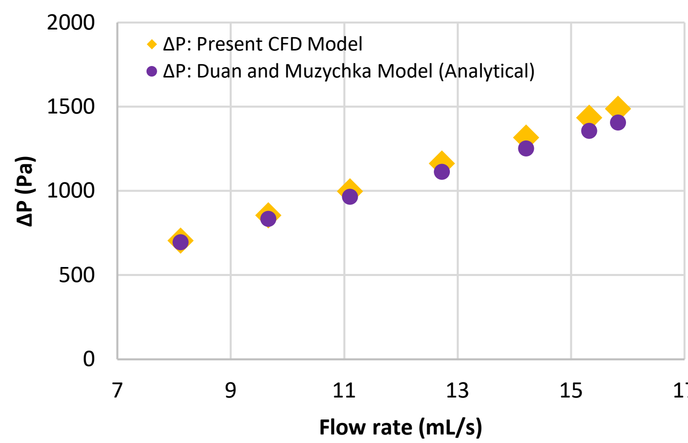

FIGURE 6:VALIDATION OF PRESENT TISE CFD MODEL (HYDRAULIC)

3. RESULTS AND DISCUSSIONS

Numerical simulations of split flow microchannel cold plates, with varying parameters (α, β and θ_{fin}), were performed, and the CFD results were compared to the new compact model predictions. For all simulations, split flow cold plates have 100 microchannels, and Table.1 shows the geometric dimensions shared by all those cold plates. The flow conditions were also all identical, with inlet fluid temperature being 300K, and the properties of the pure water and copper used in all simulations are provided in Table.2. The applied heat flux at the bases of all cold plates was $q''_B = 27W/cm^2$.

The CFD results, including the cold plate thermal resistance, defined in Eqn. 44, and pressure drop, defined in Eqn. 43, were used in the analytical model validation.

TABLE 1: GEOMETRIC DIMENSIONS SHARED BY ALL SIMULATED COLD PLATES

L(mm)	W (mm)	b (μm)	H_b (mm)	t (mm)	N_T
23.6	27	167	1.35	0.1	100

TABLE 2: THERMAL-PHYSICAL PROPERTIES OF WATER AND COPPER AT 300K

Material	ρ (kg/m³)	μ (kg/m. s)	c_p (J/kg. K)	k (W/m. K)
Water	997	0.000855	4179	0.613
Copper	8978		381	388

$$R_{bs} = \frac{(T_{B,avg} - T_{m_i})}{\dot{q}_B} \tag{44}$$

3.1 Varying Jet Slot Aspect ratio, β

Numerical simulations for generic vertical-fin split flow or TISE microchannel cold plates, with jet slot aspect ratios (β) varied from 0.1 to 0.5, as summarized in Table.3, were performed, while varying the flow rates and keeping the fin height (H = 2mm) constant. The pertinent computational domain, with boundary conditions, is provided in Fig.7.

TABLE 3: DIMENSIONS FOR COLD PLATES (VARYING β)

β	W_j (mm)	H_{fin}(mm)	θ_{fin}
0.1	2.36	2	90°
0.5	11.80	2	90°

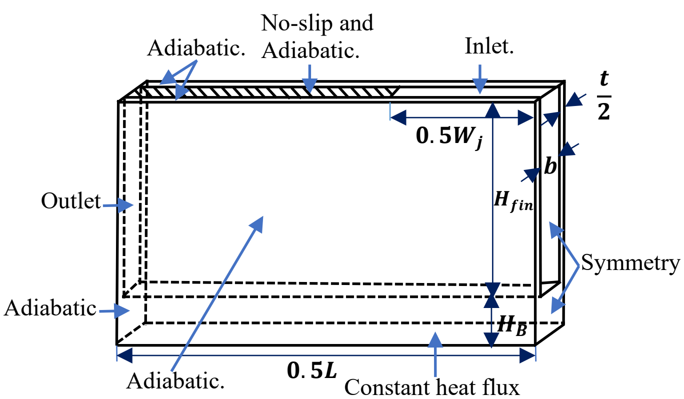

FIGURE 7: COMPUTATIONAL DOMAIN FOR GENERIC TISE CONFIGURATION WITH BOUNDARY CONDITIONS

Case for $\beta = 0.1$

From Fig.8, there is good agreement between the generic split flow (TISE) CFD model and the proposed compact isothermal model, with the maximum error of 15% registered at the lowest flow rate. Also, from Fig.9, there is excellent agreement between the pressure drop of the generic TISE cold plate and that predicted by the current proposed compact hydraulic models, with a maximum error of 8.03%. On average, to obtain a given data point on both Figs. 8 and 9, it took a millisecond for the proposed analytical models, where as a minimum of 3 minutes of computational time was needed for the TISE CFD model.

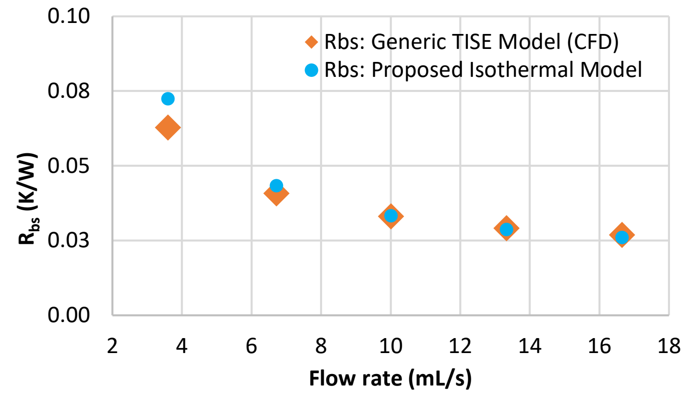

FIGURE 8: THERMAL RESISTANCE OF TISE COLD PLATE (β = 0.1)

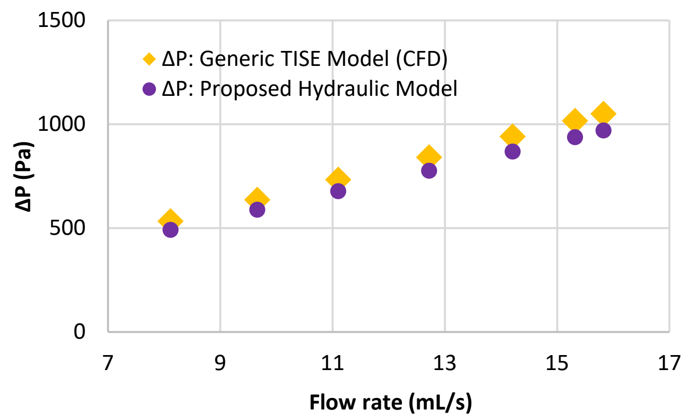

FIGURE 9: PRESSURE DROP OF TISE COLD PLATE (β = 0.1)

Case for $\beta = 0.5$

From Fig.10, there is excellent agreement between the generic split flow or TISE model and prediction from proposed compact isothermal model, with the maximum error of 10.11% registered at the lowest flow rate. There is excellent agreement between the pressure drop of the generic TISE cold plate and proposed compact hydraulic models, as shown in Fig.11, with a maximum error of 7.08%.

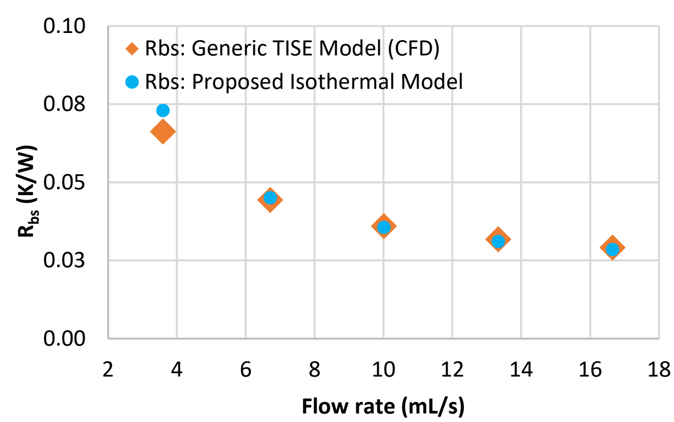

FIGURE 10: THERMAL RESISTANCE OF TISE COLD PLATE (β = 0.5)

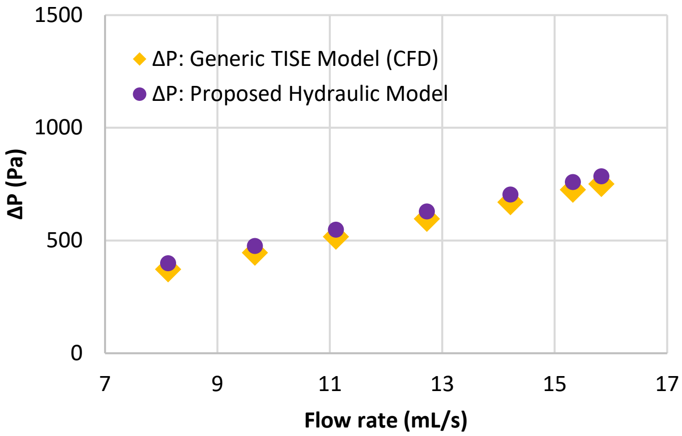

FIGURE 11: PRESSURE DROP OF TISE COLD PLATE (β = 0.5)

3.2 Variable channel aspect ratio, α

The results of thermal resistance and pressure drop from numerical simulations are presented, where for each generic vertical-fin split flow cold plate with a given fin height, the jet slot aspect ratio (β) was varied, while keeping the flow rate constant. Key geometric dimensions of the generic TISE cold plates are provided in Table.4. The computation domain for these simulations and boundary conditions are again shown in Fig.7.

TABLE 4: DIMENSIONS OF COLD PLATES (VARIABLE α)

α	$H_{fin}(mm)$	θ_{fin}	β
6	1	90°	0.1, 0.25 and 0.5
24	4	90°	0.1, 0.25 and 0.5

Case for α = 6

As illustrated in Fig.12, for all the three jet slot aspect ratios or β′s varied for the aspect ratio, α = 6, there is excellent agreement between the thermal resistance from the numerical simulations and the prediction from the proposed isothermal model, with mean error of 2.65%. Also, there is good agreement between pressure drop from the numerical simulations and the proposed hydraulic model, as shown in Fig.13, with a maximum error of 11.31%.

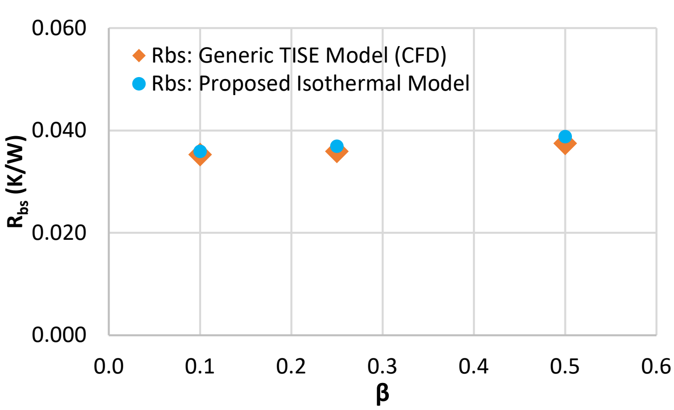

FIGURE 12: THERMAL RESISTANCE OF TISE COLD PLATE (α = 6)

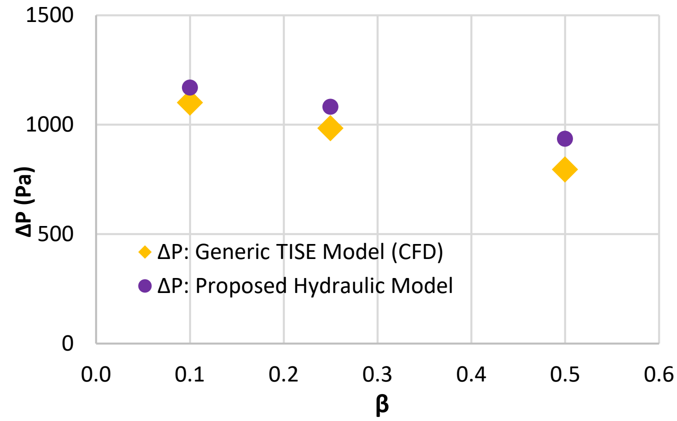

FIGURE 13: PRESSURE DROP OF TISE COLD PLATE (α = 6)

Case for α = 24

From Fig.14, for all the three jet slot aspect ratios or β′s varied for α = 24, there is a good agreement between thermal resistance data from the numerical simulations and that estimated by the proposed isothermal model, with a mean error of 16.29%. Also, there is good agreement between the pressure drop data from numerical simulations and that predicted by the proposed hydraulic model, with a mean error of 9.79%, as shown in Fig.15.

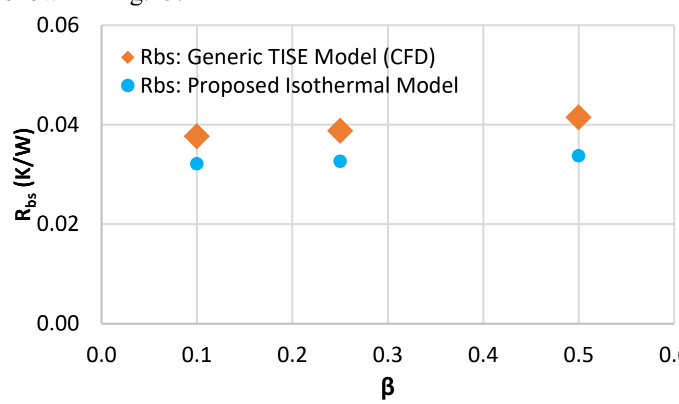

FIGURE 14: THERMAL RESISTANCE OF TISE COLD PLATE (α = 24) AT 10.01mL/s

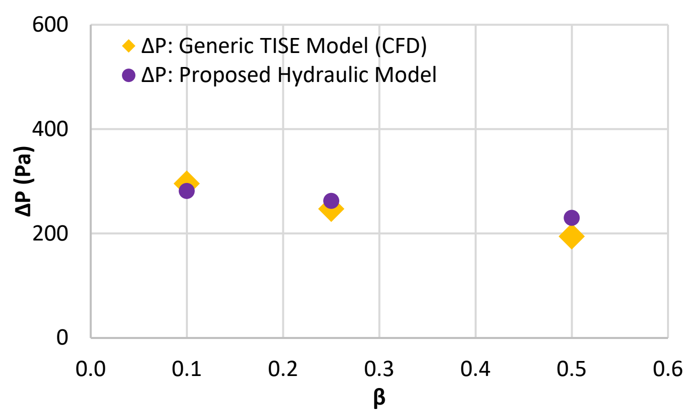

FIGURE 15: PRESSURE DROP OF TISE COLD PLATE (α = 24) AT 8.12mL/s

3.3 Variable fin tilt angles, θ_{fin}

The predictions from the compact models are compared to the results of thermal resistance and pressure drop from numerical simulations for split flow cold plates with varying fin tilt angles, $\theta_{\text{fin}} = 45°\ and\ 65°$. The computational domain and boundary conditions for these simulations are shown in Fig.16. Also, vital geometric dimensions of the generic split flow tilted-fin cold plates considered are given in Table.5.

TABLE 5: DIMENSIONS OF COLD PLATES (VARIABLE θ_{fin})

θ_{fin}	β	W_j (mm)	$H_{fin}(mm)$
45°	0.17	4	2
90°	0.17	4	2

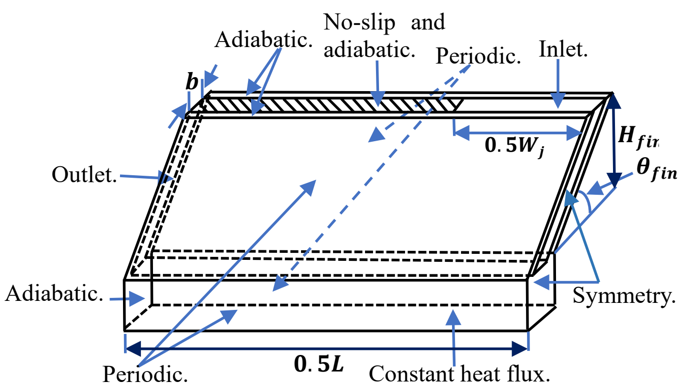

FIGURE 16: COMPUTATIONAL DOMAIN FOR TILTED-FIN SPLIT FLOW (TISE) CONFIGURATION WITH BOUNDARY CONDITIONS.

Case for $\theta_{fin} = 45°$

There is good agreement between the thermal resistance from numerical simulations on the 45°-tilted-fin generic TISE cold plate model and the proposed isothermal model, with the maximum error of 15.46%, registered at the highest flow rate, as shown in Fig.17. From Fig.18, there is an excellent agreement between the pressure drop of the 45°-tilted-fin generic TISE cold plate and the prediction from currently proposed hydraulic model, with the maximum error of 7.81%.

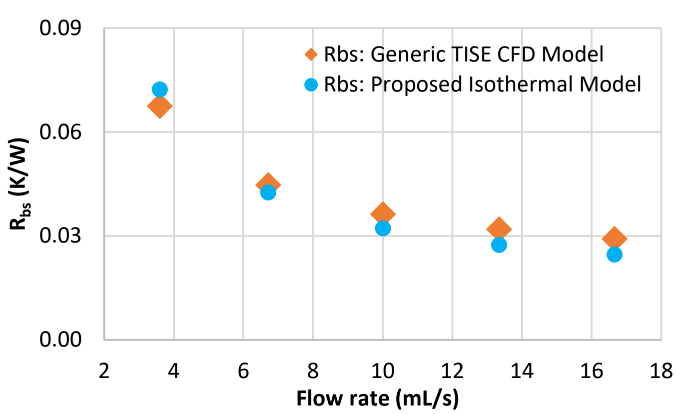

FIGURE 17: THERMAL RESISTANCE OF TISE COLD PLATE ($\theta_{fin} = 45°$)

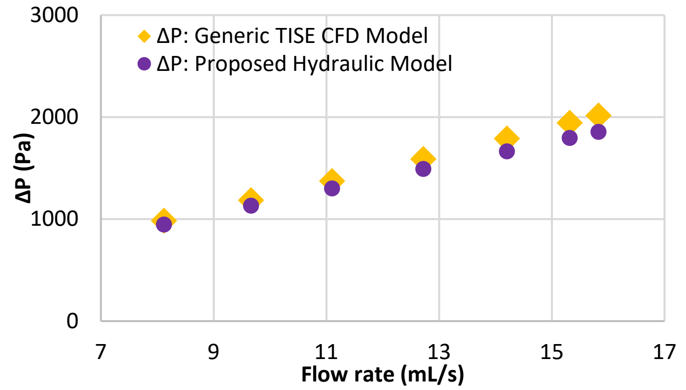

FIGURE 18: PRESSURE DROP OF TISE COLD PLATE ($\theta_{fin} = 45°$)

Case for $\theta_{fin} = 65°$

From Fig.19, good agreement is registered between thermal resistance from numerical simulations on 65°-tilted-fin generic TISE cold plate CFD model and the proposed isothermal model, with the maximum error of 14.20% obtained at the lowest flow rate. Also, excellent agreement is recorded between the pressure drop of the tilted-fin generic TISE cold plate and that estimated by the proposed hydraulic models, with the maximum error of 6.89% obtained at the largest flow rate, as shown in Fig.20.

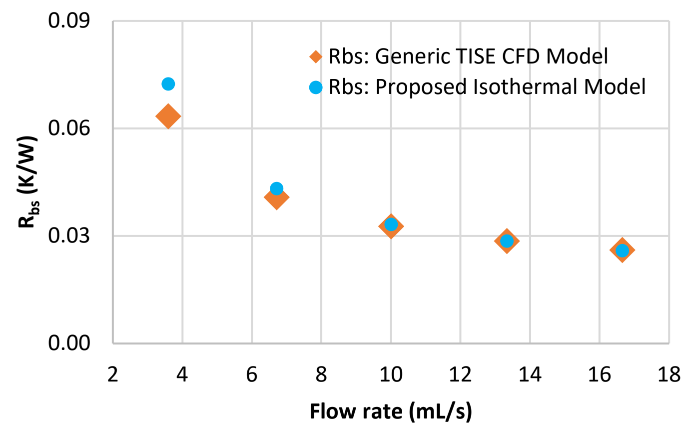

FIGURE 19: THERMAL RESISTANCE OF TISE COLD PLATE ($\theta_{fin} = 65°$)

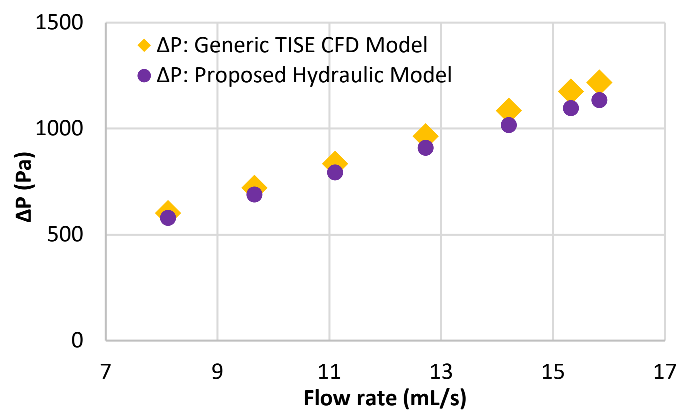

FIGURE 20: PRESSURE DROP OF TISE COLD PLATE ($\theta_{\text{fin}} = 65°$)

4. CONCLUSIONS

In this article, novel compact physics-based thermal-hydraulic analytical models for split flow (jet impingement) liquid-cooled microchannel cold plates were derived basing on the presently proposed equivalent parallel flow concept. Both thermal resistance and pressure drop of the split flow cold plates, obtained from CFD simulations, were predicted well by the new compact analytical models, over a wide range of parameters. The model accuracy slightly decreases at very high channel aspect ratio (α) for only thermal resistance predictions. For future studies, temperature dependent thermal-physical properties of the liquid coolant should be considered in the modeling. It is also recommended that experimental work with deionized (DI) water and 25% propylene glycol solution (coolant) is conducted on split flow cold plates to further validate the proposed compact analytical models. Split flow cold plates with jet slot aspect ratios, β's larger than 0.5 should also be studied.

ACKNOWLEDGEMENTS

The authors would like to recognize the National Science Foundation Industry University Collaborative Research Center (NSF IUCRC) for funding this work under Grant No. IIP-1738782. Any opinions, findings, and conclusions or recommendations expressed in this article are solely the responsibility of the authors and do not necessarily represent the official views of the NSF.

REFERENCES

[1] Z. Duan and Y. Muzychka, "Pressure Drop of Impingement Air Cooled Plate Fin Heat Sinks," *Journal of Electronic Packaging,* vol. 129, 2007.

[2] S. S. Kang, and M. F. Holahan, "Impingement Heat Sinks for Air Cooled High Power Electronic Modules," in *1995 National Heat Transfer Conference*, 1995.

[3] M. F. Holahan, S. S. Kang and A. Bar-Cohen, "A Flowstream Based Analytical Model of Design of Parallel Plate Heat Sinks," in *A Flowstream Based Conference*, Houston, Texas, USA, 1996.

[4] C. R. Biber, "Pressure drop and heat transfer in an isothermal channel with impinging flow," *in IEEE Transactions on Components, Packaging, and Manufacturing Technology: Part A,* vol. 20, no. 4, pp. 458-462, 1997.

[5] I. S. Issa and A. Ortega, "Experimental Measurements of the Flow and Heat Transfer of a Square Jet Impinging on an Array of Square Pin Fins," in *Proc IMECE2002*, New Orleans, Louisiana, 2002.

[6] F. E. O. Gutiérrez and A. Ortega, "Hydraulic and Thermal Characterization of Parallel Plate Fin Heat Sinks Under Side Inlet - Side Exit Flow Configuration, and Top Inlet-Side Exit Flow Configuration with and Without Top Flow Bypass," University of Arizona, Arizona, USA, 2005.

[7] M. K. Sung and I. Mudawar, "Single-phase and two-phase cooling using hybrid micro-channel/slot-jet module," *International Journal of Heat and Mass Transfer,* vol. 51, p. 3825–3839, 2008.

[8] Y. Hadad, N. Fallahtafti, L. Choobineh , C. H. Hoang, V. Radmard, P. R. Chiarot, B. Sammakia, "Performance Analysis and Shape Optimization of an Impingement Microchannel Cold Plate," *IEEE TRANSACTIONS ON COMPONENTS, PACKAGING AND MANUFACTURING TECHNOLOGY,* vol. 10, no. 8, pp. 1304-1319, 2020.

[9] Y. Hadad, S. Rangararajan, K. Nemati, B. Ramakrishnann, R. Pejman, P. R. Chiarot, B. Sammakia,, "Performance analysis and shape optimization of a water-cooled impingement micro-channel heat sink including manifolds," *International Journal of Thermal Sciences,* vol. 148, no. ISSN 1290-0729, p. 106145, 2020.

[10] B. Ramakrishnan, Y. Hadad, S. Alkharabsheh, P. R. Chiarot and B. Sammakia, "Thermal Analysis of Cold Plate for Direct Liquid Cooling of High Performance Servers," *Journal of Electronic Packaging,* vol. 141, 2019.

[11] S. Kandlikar, S. Garimella, D. Li, S. Colin, and M. King,, "Heat Transfer and Fluid Flow in Minichannels and Microchannels," 2014.

[12] D. Copeland, "Optimization of parallel plate heatsinks for forced convection," in *Sixteenth Annual IEEE Semiconductor Thermal Measurement and Management Symposium (Cat. No.00CH37068)*, San Jose, CA, 2000.

[13] D. Kisitu, "Approximate thermal-hydraulic analytical models for laminar microchannel impingement liquid-cooled cold plates for data center thermal management.," MSc. Thesis, Villanova University, Villanova, USA, 2021.

[14] S. Lee, "Calculating Spreading Resistance in Heat Sinks," Electronics Cooling, 1998.

[15] W. M, Kays and A. L. London, Compact Heat Exchangers, 3rd ed, New York, NY, USA: McGraw Hill, 1984.

[16] A. Rohatgi, "WebPlotDigitizer: Version 4.4," Pacifica, CA, USA, 2020.

